

Article

Kinetic Analysis of the Gas-Phase Reactions of Methyl *Tert*-Butyl Ether with the OH Radical in the Presence of NO_x

*André Silva Pimentel**, and *Graciela Arbilla*

*Departamento de Físico-Química, Instituto de Química, Universidade Federal do Rio de Janeiro, Centro de Tecnologia – Bloco A – Sala 408, Cidade Universitária, 21949-900 Rio de Janeiro - RJ, Brazil; *e-mail pimentel@iq.ufrj.br*

Received: June 22, 1998

Um mecanismo explícito para a reação do metil-terc-butil-éter (MTBE) com radicais OH, numa mistura NO_x – ar, foi simulado resolvendo as equações diferenciais ordinárias usando o método Runge-Kutta-4-semi-implícito. Os resultados simulados são consistentes com os dados experimentais publicados e o modelo explica as principais vias de reação para a oxidação do MTBE com radicais OH na presença de NO_x – ar. Usando uma análise dos autovetores e autovalores dos coeficientes de sensibilidade, para todas as espécies químicas envolvidas em diferentes tempos de reação, foi extraída informação cinética do sistema. Este método foi utilizado para reduzir o modelo cinético de forma objetiva. Foi utilizado, também, o método tradicional de análise de velocidade de produção (ROPA) para estudar a importância relativa das reações individuais. Usando a informação da análise de componente principal e da análise de velocidade de produção, foram identificadas as principais reações individuais.

An explicit chemical mechanism for the reaction of methyl tert-butyl ether (MTBE) with OH radicals in NO_x-air systems, was simulated by solving the corresponding ordinary differential equations using Runge-Kutta-4-semi-implicit method. The simulated results are consistent with the published experimental data and the model accounts for all the major pathways by which MTBE reacts in NO_x-air systems. An eigenvalue-eigenvector analysis is used to extract meaningful kinetic information from linear sensitivity coefficients computed for all species of the chemical mechanism at several time points. This method is used to get an objective condition for constructing a minimal reaction set. Also, a classic method called rate of production analysis (ROPA) was used for the study of the reactions relevance. Using the principal component information as well as the rate of production analysis the main paths of reaction are identified and discussed.

Keywords: *principal component analysis, eigenvalue-eigenvector analysis, rate of production analysis, methyl tert-butyl ether*

Introduction

Numerical integration of the coupled differential equations, which describe a reaction system, is becoming an important tool in chemical kinetics. The results and conditions obtained from such kinetic models are largely dependent on the selection of the elementary steps and their rate coefficients. For complex models, it is frequently difficult to assess the relative importance of each step or to explain certain features of the system kinetic behavior.

In order to assess the relationship between the model results and kinetic parameters and to evaluate which parts of the model are of particular importance, some sensitivity analysis is usually required¹⁻⁶.

In this work, the gas-phase reactions of methyl tert-butyl ether (hereafter MTBE, CH₃OC(CH₃)₃) with OH radicals in NO_x-air systems are simulated and the relative importance of the elementary processes is carried out by an eigenvalue-eigenvector analysis of the linear sensitivity coefficients called Principal Component Analysis⁷.

Like other oxygenated organic compounds, including alcohols and ethers, MTBE is oxidized in ambient air by OH radical-initiated reactions⁸⁻²¹. The secondary products formed from MTBE may produce ozone in a complex sequence of photochemical reactions, involving volatile organic compounds and nitrogen oxides.

Some experimental studies have been conducted for the MTBE reaction with OH radicals^{12-14, 19-20}. The results of Tuazon *et al.*¹⁹ and Carter *et al.*²⁰ are the most complete data set for MTBE reactions. These references report the same experiments. The authors measured and identified the products of MTBE oxidation, obtaining directly quantitative yields for the tert-butyl formate (TBF, (CH₃)₃CO-CHO), formaldehyde (HCHO), acetone (CH₃C(O)CH₃) and methyl acetate (CH₃C(O)OCH₃). They also discussed and recommend a mechanism to represent the MTBE + OH chemistry. Nevertheless, to our knowledge, a sensitivity analysis of the mechanism has not been done up to now.

In this paper the initial conditions for the simulations were those of the laboratory smog chamber experiments from Tuazon *et al.*¹⁹ in order to compare the calculated and experimental results.

The Chemical Mechanism

As previously discussed^{19-20, 22-24} MTBE reacts essentially with OH radicals by H-atom abstraction, with an overall rate constant of 2.80 × 10⁻¹² cm³ molecule⁻¹ s⁻¹ at 298 K.

The present chemical mechanism considers 30 species and 41 reactions. It was proposed on the basis of reliable, previous models²⁵⁻³⁰ and of the known MTBE and CH₃O_x radicals chemistry. Thermal rate constants were either taken from literature^{22-24, 29-32} or estimated by comparison with similar compounds^{22-24, 32}. The photochemical reaction rates were estimated on the basis of the ethyl nitrite photodecomposition experimental data¹⁹⁻²⁰. The chemical mechanism is listed in Table 1.

Methodology

Numerical simulation and principal component analysis of kinetic models is fully described in the literature^{6-7, 33-35}. Briefly, the kinetic model can be represented by a set of ordinary kinetic differential equations,

$$\frac{\partial c(t)}{\partial t} = f(k, c(t))$$

where $c(t)$ is the n-vector of species concentrations with $c(t = 0) = c^0$ and k is the m-vector of kinetic parameters. A change in the kinetic parameters from k^0 to k at time t_1 causes a change in the solution of the system at a time t_2 (with $t_2 > t_1$). The effect of the parameter change on the solution can be expressed through the first order local sensitivity coefficients defined as

$$S_{ij}(k^0, c^0, t_1, t_2) = \frac{\partial c_i(t_2)}{\partial k_j}$$

In the first order approximation, the concentration sensitivity defined above represents the magnitude of the deviation in the concentration of species i at time t_2 due to the differential variation of the parameter of reaction j at time t_1 from value k_j^0 to k_j . For the present model, the parameters k_j are the thermal rate constants and photochemical coefficients.

Sensitivity coefficients are normalized in order to eliminate their dependence on the dimensions of the kinetic model. The sum of the squares of the normalized sensitivities is called overall sensitivity. A convenient way to understand the sensitivity results is in terms of the eigenvalues and eigenvectors of the matrix $S^T S$, where S is the array of normalized sensitivity coefficients. The methodology of principal component analysis is fully discussed in the literature⁵⁻⁷.

The classic method for the study of the reactions relevance is the rate of production analysis called ROPA³⁶⁻³⁷. Although the combination of species reduction and rate sensitivity analysis⁶ seems to be a more effective way for this purpose, the rate of production analysis is still an important method for the exploration of important reaction pathways. The rate of production analysis requires the calculation of the P_{ij} matrix elements³⁸, which show the contribution of reaction j to the rate of production of species i .

Results and Discussions

The full mechanism and rate constants are presented in Table 1. The reduced mechanism was obtained after elimination of the non-important reactions (denoted by # in Table 1) on the basis of the principal component analysis described below. The rank of reactions ordered by overall sensitivities and rates is shown in Table 2. We calculated normalized sensitivities for all species at time points 1, 2, 3, 4, 5 and 6 min. Eigenvalues of $S^T S$ and the corresponding eigenvectors are listed in Table 3.

In the conditions of the modelling, the main source of hydroxyl radicals is the reaction (5) (HO₂ + NO → OH + NO₂) which follows the photolysis of the ethyl nitrite (CH₃CH₂ONO + $h\nu$ → CH₃CH₂O + NO) and the oxidation of the CH₃CH₂O radicals (CH₃CH₂O + O₂ → CH₃CHO + HO₂). Reaction (5) accounts for ca. 95% of OH radical formed and the only significant sources of NO are the photodecomposition of ethyl nitrite (46%) and NO₂ (54%), reactions (27) and (10), respectively. Since we had no data on photolysis light intensities during the experiments, the ethyl nitrite photodecomposition coefficient was estimated from experimental data (Fig. 1) and values, which gave consistent results for other photodecompositions, were used. The photolysis rates were also consistent with the

Table 1. Chemical mechanism for gas-phase reactions of MTBE with the OH radical in the presence of NO_x.

Reactions	Rate Constants at 298 K Units of molecule, cm ³ , s
1) HONO + OH → H ₂ O + NO ₂	k ₁ = 4.86 × 10 ⁻¹²
2) OH + HNO ₃ → H ₂ O + NO ₃	k ₂ = 1.50 × 10 ⁻¹³
3) NO + OH → HONO	k ₃ ^a = 1.12 × 10 ⁻¹¹
4) OH + NO ₂ → HNO ₃	k ₄ ^a = 1.34 × 10 ⁻¹¹
5) HO ₂ + NO → OH + NO ₂	k ₅ = 8.28 × 10 ⁻¹²
6) NO + O ₃ → NO ₂ + O ₂	k ₆ = 1.81 × 10 ⁻¹⁴
7) NO + NO ₃ → 2 NO ₂	k ₇ = 2.60 × 10 ⁻¹¹
8) NO ₂ + O ₃ → NO ₃ + O ₂	k ₈ = 3.23 × 10 ⁻¹⁷
9) HONO + <i>hν</i> → OH + NO	j ₉ = 1.63 × 10 ⁻³
10) NO ₂ + <i>hν</i> + (O ₂) → NO + O ₃	j ₁₀ = 4.26 × 10 ⁻³
11) HCHO + OH + (O ₂) → HO ₂ + CO + H ₂ O	k ₁₁ = 9.57 × 10 ⁻¹²
12) CH ₃ CHO + OH + (O ₂) → CH ₃ CO ₃ + H ₂ O	k ₁₂ = 1.58 × 10 ⁻¹¹
13) CH ₃ O + (O ₂) → HCHO + HO ₂	k ₁₃ = 4.59 × 10 ⁴
14) CH ₃ O ₂ + NO → NO ₂ + CH ₃ O	k ₁₄ = 7.68 × 10 ⁻¹²
15) CH ₃ CO ₃ + NO + (O ₂) → NO ₂ + CH ₃ O ₂ + CO ₂	k ₁₅ ^a = 9.98 × 10 ⁻¹²
16) CH ₃ CO ₃ + NO ₂ → CH ₃ CO ₃ NO ₂	k ₁₆ = 3.63 × 10 ⁻¹²
#17) CH ₃ CO ₃ NO ₂ → CH ₃ CO ₃ + NO ₂	k ₁₇ = 1.81 × 10 ⁻⁴
18) CH ₃ CH ₂ O + O ₂ → CH ₃ CHO + HO ₂	k ₁₈ = 9.48 × 10 ⁻¹⁵
#19) CH ₃ CH ₂ O + NO → CH ₃ CH ₂ ONO	k ₁₉ = 4.40 × 10 ⁻¹¹ (k _∞)
20) CH ₃ OC(CH ₃) ₃ + OH + (O ₂) → H ₂ O + 0.80 (CH ₃) ₃ COCH ₂ O ₂ + 0.20 CH ₃ OC(CH ₃) ₂ CH ₂ O ₂	k ₂₀ ^b = 2.83 × 10 ⁻¹²
21) (CH ₃) ₃ COCH ₂ O ₂ + NO → (CH ₃) ₃ COCH ₂ O + NO ₂	k ₂₁ ^c = 8.90 × 10 ⁻¹²
22) (CH ₃) ₃ COCH ₂ O + (O ₂) → (CH ₃) ₃ COCHO + HO ₂	k ₂₂ ^d = 3.80 × 10 ⁶
23) CH ₃ OC(CH ₃) ₂ CH ₂ O ₂ + NO → CH ₃ OC(CH ₃) ₂ CH ₂ O + NO ₂	k ₂₃ ^c = 1.50 × 10 ⁻¹⁴
24) CH ₃ OC(CH ₃) ₂ CH ₂ O + (O ₂) → CH ₃ OC(CH ₃) ₂ O ₂ + HCHO	k ₂₄ ^c = 2.00 × 10 ⁷
25) CH ₃ OC(CH ₃) ₂ O ₂ + NO → CH ₃ OC(CH ₃) ₂ O + NO ₂	k ₂₅ ^c = 8.90 × 10 ⁻¹²
26) CH ₃ OC(CH ₃) ₂ O + (O ₂) → 0.88 CH ₃ C(O)OCH ₃ + 0.88 CH ₃ O ₂ + 0.12 CH ₃ C(O)CH ₃ + 0.12 CH ₃ O	k ₂₆ ^c = 9.68 × 10 ⁴
27) CH ₃ CH ₂ ONO + <i>hν</i> → CH ₃ CH ₂ O + NO	j ₂₇ ^c = 0.54 × 10 ⁻³
#28) 2 OH → H ₂ O ₂	k ₂₈ = 1.14 × 10 ⁻¹¹
#29) H ₂ O ₂ + OH → H ₂ O + HO ₂	k ₂₉ = 1.70 × 10 ⁻¹²
30) HO ₂ + HO ₂ → H ₂ O ₂ + O ₂	k ₃₀ = 7.73 × 10 ⁻¹²
31) HO ₂ + NO ₂ → HO ₂ NO ₂	k ₃₁ = 2.33 × 10 ⁻¹²
32) HO ₂ NO ₂ → HO ₂ + NO ₂	k ₃₂ = 1.68 × 10 ⁻¹
33) NO ₂ + NO ₃ → N ₂ O ₅	k ₃₃ = 6.56 × 10 ⁻¹³
34) N ₂ O ₅ → NO ₂ + NO ₃	k ₃₄ = 2.27 × 10 ⁻²
35) CH ₃ O + NO → CH ₃ ONO	k ₃₅ = 2.13 × 10 ⁻¹¹
#36) CH ₃ O + NO ₂ → CH ₃ ONO ₂	k ₃₆ = 8.75 × 10 ⁻¹²
37) CH ₃ O ₂ + NO ₂ → CH ₃ O ₂ NO ₂	k ₃₇ = 2.93 × 10 ⁻¹²
38) CH ₃ O ₂ NO ₂ → CH ₃ O ₂ + NO ₂	k ₃₈ = 1.698
#39) HCHO + (2 O ₂) + <i>hν</i> → 2 HO ₂ + CO	j ₃₉ = 1.76 × 10 ⁻⁵
#40) HCHO + <i>hν</i> → H ₂ + CO	j ₄₀ = 2.66 × 10 ⁻⁵
#41) CH ₃ CHO + (2 O ₂) + <i>hν</i> → CH ₃ O ₂ + HO ₂ + CO	j ₄₁ = 3.53 × 10 ⁻⁶

a- Ref. 32; b- Ref. 24; c- Estimated; d- Refs. 22 and 23; e- Ref. 33; # Non-important Reactions

Table 2. Rank of reactions by overall sensitivity and rates.

Rank	Reaction	Overall Sens.*	Reaction	Rates**
1	27	$3.61 \times 10^{+02}$	10	$5.07 \times 10^{+11}$
2	20	$1.04 \times 10^{+02}$	6	$5.03 \times 10^{+11}$
3	3	$5.27 \times 10^{+01}$	5	$2.18 \times 10^{+11}$
4	4	$4.36 \times 10^{+01}$	27	$1.26 \times 10^{+11}$
5	5	$2.78 \times 10^{+01}$	18	$1.25 \times 10^{+11}$
6	12	$1.67 \times 10^{+01}$	31	$1.15 \times 10^{+11}$
7	10	$1.35 \times 10^{+01}$	32	$1.12 \times 10^{+11}$
8	6	$1.34 \times 10^{+01}$	4	$1.07 \times 10^{+11}$
9	14	$1.20 \times 10^{+01}$	20	$6.27 \times 10^{+10}$
10	7	$1.18 \times 10^{+01}$	21	$5.01 \times 10^{+10}$
11	15	8.69	22	$5.01 \times 10^{+10}$
12	8	7.70	3	$4.79 \times 10^{+10}$
13	18	6.01	12	$4.20 \times 10^{+10}$
14	26	6.00	14	$3.64 \times 10^{+10}$
15	24	6.00	13	$3.60 \times 10^{+10}$
16	22	6.00	9	$2.85 \times 10^{+10}$
17	25	6.00	37	$2.59 \times 10^{+10}$
18	21	6.00	38	$2.58 \times 10^{+10}$
19	23	6.00	15	$2.53 \times 10^{+10}$
20	37	5.98	16	$1.72 \times 10^{+10}$
21	38	5.91	26	$1.25 \times 10^{+10}$
22	33	5.90	24	$1.25 \times 10^{+10}$
23	16	5.77	25	$1.25 \times 10^{+10}$
24	31	5.70	23	$1.25 \times 10^{+10}$
25	13	5.31	11	$9.61 \times 10^{+09}$
26	32	5.19	1	$5.66 \times 10^{+09}$
27	30	4.24	7	$1.89 \times 10^{+09}$
28	9	1.73	8	$1.68 \times 10^{+09}$
29	34	1.55	19	$1.54 \times 10^{+09}$
30	2	4.89×10^{-01}	35	$1.07 \times 10^{+09}$
31	1	4.63×10^{-01}	36	$8.17 \times 10^{+08}$
32	19	2.17×10^{-01}	17	$4.12 \times 10^{+08}$
33	28	1.66×10^{-01}	40	$3.98 \times 10^{+08}$
34	11	7.37×10^{-02}	39	$2.64 \times 10^{+08}$
35	35	6.52×10^{-02}	2	$2.46 \times 10^{+08}$
36	36	5.23×10^{-03}	41	$1.40 \times 10^{+08}$
37	39	1.10×10^{-03}	33	$8.90 \times 10^{+07}$
38	17	1.03×10^{-03}	34	$5.71 \times 10^{+07}$
39	29	8.38×10^{-04}	30	$1.32 \times 10^{+06}$
40	41	7.00×10^{-04}	28	$5.12 \times 10^{+04}$
41	40	4.56×10^{-05}	29	$2.66 \times 10^{+04}$

* undimensional; ** Units of molecule, cm³, s.

Eigenvalues	6.00	6.00	6.00	6.00	5.98	3.85	3.26	2.91	2.71	1.95
Eigenvectors [@]										
1	(26) .814	(24) -.681	(25) -.728	(23) -.806	(22) -.429	(14) .492	(18) .623	(33) -.686	(16) .799	(23) .405
2	(24) -.420	(22) .676	(21) .621	(21) .475	(24) -.429	(37) .487	(12) -.372	(7) -.435	(14) -.319	(21) .405
3	(22) -.391	(21) -.226	(22) .218	(25) .332	(26) -.426	(38) -.484	(27) .311	(8) .357	(15) .318	(25) .405
4	(21) .069	(25) .152	(24) -.140	(22) .093	(23) .326	(13) -.391	(3) .272	(34) .352	(13) -.221	(14) .272
5	(25) -.066	(23) .074	(23) .106	(24) -.079	(21) .324	(16) .281	(14) .219	(18) -.123	(3) .132	(22) .270
6			(26) -.078		(25) .324	(18) -.110	(33) -.203	(3) -.107	(37) -.132	(24) .270
7					(13) -.313	(15) -.081	(4) .201	(10) -.104	(38) .131	(26) .270
8					(18) -.151	(33) .072	(5) .197	(6) .104	(12) -.130	(15) .213
9					(16) -.061	(5) -.067	(20) -.129	(2) .083	(33) -.098	(4) -.173
10						(20) .058	(22) -.123	(4) -.081	(18) .088	(13) .157
11							(24) -.123	(16) -.075	(7) -.075	(7) .145
12							(26) -.123	(27) -.071	(8) .059	(5) .129
13							(16) -.122	(12) .060	(27) .055	(6) .096
14							(34) .102		(34) .053	(10) -.096
15							(15) .093			(31) -.087
16							(30) -.080			(30) -.087
17							(37) .070			(8) -.086
18							(38) -.070			(12) -.084
19							(1) -.062			(32) .080
20							(10) -.055			(3) -.076
21							(6) .054			(20) .073
22										(33) -.069
23										(2) -.057

Eigenvalues	1.56	8.93×10^{-1}	5.54×10^{-1}	2.44×10^{-1}	6.58×10^{-2}	3.99×10^{-2}	2.75×10^{-2}	1.69×10^{-2}	1.21×10^{-2}	3.25×10^{-3}
Eigenvectors [@]										
1	(20) -.510	(30) .846	(15) .566	(9) -.623	(34) .656	(11) -.786	(1) .938	(2) .657	(28) -.863	(35) -.928
2	(3) -.473	(5) .352	(12) .521	(15) .233	(11) -.484	(34) -.475	(34) .243	(8) -.465	(2) -.300	(11) .267
3	(4) -.463	(31) .179	(14) .309	(3) -.192	(33) .337	(33) -.238	(33) .103	(28) -.402	(8) .219	(36) .125
4	(12) -.357	(32) -.172	(13) .293	(12) .157	(2) .281	(35) -.211	(28) .092	(34) -.268	(35) -.176	(28) .124
5	(9) .162	(28) .159	(9) .235	(4) -.139	(1) -.256	(28) .156	(11) -.085	(7) -.238	(11) -.165	(32) -.088
6	(30) .158	(20) .123	(4) .150	(14) .120	(8) -.207	(15) -.068	(9) .083	(33) -.148	(30) .153	(31) -.085
7	(15) .127	(3) .110	(30) .122	(11) -.098	(35) -.129	(1) .066	(35) .072	(11) .129	(7) .112	(19) -.081
8	(5) .116	(9) -.093	(16) .112	(13) .096	(7) -.110	(12) -.059	(19) -.052	(1) .105	(1) .086	(17) -.080
9	(31) .089	(15) -.082	(22) -.096	(1) .095		(19) -.052		(30) .081	(29) -.071	(1) .061
10	(32) -.085	(4) .061	(24) -.095	(20) -.090		(30) -.050			(34) .056	
11	(23) -.080	(23) .054	(26) -.095	(22) -.083						
12	(25) -.080	(25) .054	(23) -.084	(24) -.083						
13	(21) -.080	(21) .054	(21) -.084	(26) -.083						
14	(24) -.062		(25) -.084	(23) -.059						
15	(22) -.062		(34) -.056	(21) -.059						
16	(26) -.062		(5) .052	(25) -.059						
17	(7) .061									
18	(16) .058									
19	(8) -.056									
20	(13) .051									

Eigenvalues	9.75×10^{-4}	4.45×10^{-4}	1.44×10^{-4}	1.19×10^{-4}	2.00×10^{-5}	1.52×10^{-5}	5.72×10^{-6}	3.23×10^{-6}	2.08×10^{-6}	1.77×10^{-6}
Eigenvectors [@]										
1	(32) .671	(19) -.911	(17) -.976	(36) .930	(38) -.673	(39) .783	(6) .551	(29) .979	(40) .706	(41) .858
2	(31) .639	(32) -.236	(19) .113	(19) .195	(37) -.669	(41) .420	(10) .548	(41) -.160	(2) -.324	(39) -.412
3	(19) -.310	(31) -.226	(39) -.106	(38) -.140	(36) -.223	(2) -.200	(2) -.336	(40) -.080	(6) -.310	(29) .142
4	(36) .179	(35) .135	(41) -.101	(37) -.139	(39) -.180	(7) -.185	(7) -.324	(28) -.075	(10) -.308	(6) .141
5	(11) .066	(36) .116	(35) .071	(39) -.127	(40) .065	(8) -.180	(8) -.317		(7) -.299	(10) .140
6		(39) -.107		(35) .097		(17) -.168	(39) -.187		(8) -.290	(40) .082
7		(17) -.082		(32) -.083		(36) .141	(41) -.182		(39) -.135	(38) .079
8		(1) -.068		(31) -.079		(38) -.135	(29) -.070		(29) .087	(37) .078
9		(28) -.053		(41) -.077		(37) -.134				(2) .068
10				(11) -.064		(19) -.083				(7) .063
11						(40) -.067				(8) .061
12						(29) .052				

[@]First entry refers to the rate constant for the reaction listed in Table 1 and second entry lists eigenvector components.

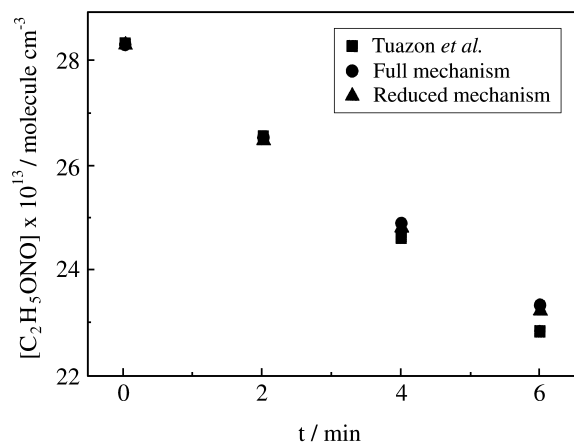
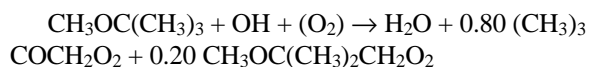


Figure 1. Simulated and experimental data for the ethyl nitrite photodecomposition as a function of reaction time.

value reported in the literature²⁰ for NO₂ photodecomposition. Also, photochemical reactions of other species, not including NO₂ photodecomposition, are of negligible importance compared with other paths. As expected the set of reactions of Table 1 accounts for the formation of the main products, *tert*-butyl formate, formaldehyde, methyl acetate, and acetone. As shown in Figs. 2 and 3, the simulated results are in reasonable agreement with experimental data, both for MTBE and the main products concentrations.

In this simulation conditions, formaldehyde is formed both from acetaldehyde, the initial product of ethyl nitrite photolysis, reaction (27), and by the sequence of reactions initiated by OH radical oxidation of MTBE:



The rate of production analysis shows that 60% of formaldehyde is formed through reaction (13), $\text{CH}_3\text{O} + (\text{O}_2) \rightarrow \text{HCHO} + \text{HO}_2$ and 40% through the reaction

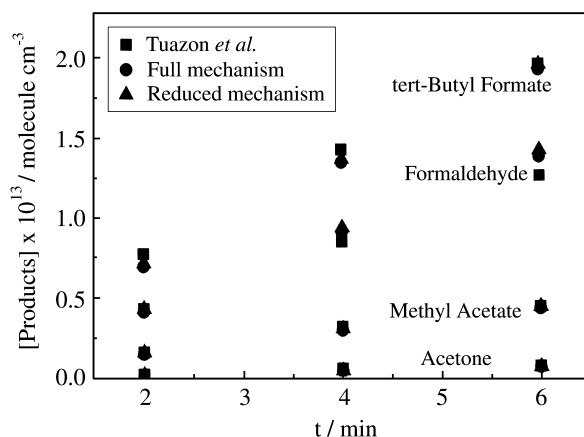


Figure 2. Simulated and experimental data for the main products of the gas-phase reactions of MTBE with the OH radical in the presence of NO_x as a function of reaction time.

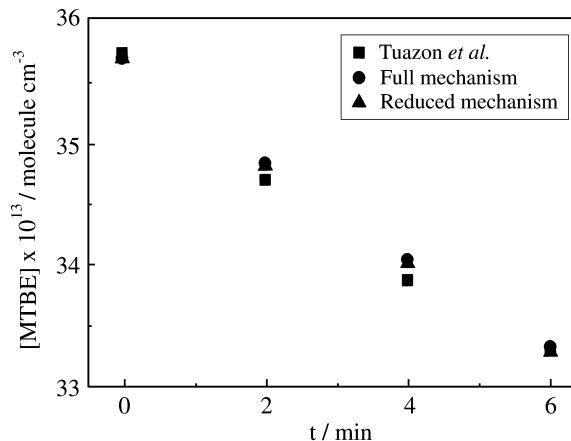


Figure 3. Simulated and experimental data for the oxidation of the MTBE as a function of reaction time.

sequence (20), (23) and (24), which involve the reaction of $\text{CH}_3\text{OC}(\text{CH}_3)_2\text{CH}_2\text{O}_2$ with NO and O₂. Under the modeling conditions, the secondary reactions of formaldehyde are of minor importance. As observed experimentally^{19,23-24}, the formed formaldehyde reacts essentially with OH radicals which are in relatively high concentrations (calculated values about 9×10^7 molecule cm⁻³). Nevertheless, the rate of this reaction path is 3.6% of the total formation rate and, in comparison with OH radical reaction (11) ($\text{HCHO} + \text{OH} + (\text{O}_2) \rightarrow \text{HO}_2 + \text{CO} + \text{H}_2\text{O}$), the photochemical decompositions (39) and (40) ($\text{HCHO} + (2 \text{O}_2) + h\nu \rightarrow 2 \text{HO}_2 + \text{CO}$ and $\text{HCHO} + h\nu \rightarrow \text{H}_2 + \text{CO}$) are of negligible importance.

According to the calculated results, 22% of formaldehyde is generated by the following sequence: ethyl nitrite photolysis, $\text{CH}_3\text{CH}_2\text{O}$ oxidation to acetaldehyde and its decomposition and, finally, oxidation of CH_3O , reactions (27), (18), (12), (15), (14) and (13). As previously stated, MTBE reaction with OH radical leads to formaldehyde (40% of total) through the sequence of reactions (20), (23) and (24) which does not involve CH_3O_x radicals. The other 60% of formaldehyde can be attributed to the subsequent reactions of ethyl nitrite photolysis products and to the sequence (20), (23), (24), (25), (26), (14) and (13) which leads to methyl acetate and formaldehyde, and by another sequence (20), (23), (24), (25), (26) and (13) which leads to acetone and formaldehyde. All these paths involve CH_3O_x radical. Since rate coefficients of many of these reactions are estimated values, these paths are subject to considerable uncertainty.

In the conditions of this simulation, the formation of acetaldehyde (Fig. 4) and peroxyacetyl nitrate (PAN) (Fig. 5) can be attributed to the photooxidation of ethyl nitrite¹⁹⁻²⁰. The main discrepancy between the experimental results and the model predictions is the much lower concentrations of calculated peroxyacetyl nitrate. The reasons for this discrepancy are not well established, but may be associated

to the large uncertainty in the related kinetic parameters. Also, other reactions which have not been considered in the present work, such as heterogeneous reactions, may be important to describe the whole system. In comparison with OH radical reaction ($\text{CH}_3\text{CHO} + \text{OH} + (\text{O}_2) \rightarrow \text{CH}_3\text{CO}_3 + \text{H}_2\text{O}$), the acetaldehyde photochemical decompositions ($\text{CH}_3\text{CHO} + (2 \text{ O}_2) + h\nu \rightarrow \text{CH}_3\text{O}_2 + \text{HO}_2 + \text{CO}$) are of negligible importance, as shown by the principal component analysis.

The 1st and 2nd principal components in Table 3 show that ethyl nitrite photodecomposition, reaction (27), oxidation of MTBE, reaction (20), and OH/NO chemistry, reactions (3), (4) and (5), are strongly coupled and are the most influential reaction sequence in the mechanism. Thus a small deviation in k_{20} or j_{27} should largely affect the simulation results.

According to the magnitude of the eigenvalues and significant entries (≥ 0.20) of the corresponding eigenvec-

tor, the individual reactions may be classified in three groups:

1) Eigenvalues λ_1 to λ_{21} are much larger than the remaining ones. Note that $\sum_{i=1}^{21} \lambda_i / \sum_{j=1}^{41} \lambda_j = 0.9976$. Prin-

cipal components ψ_1 to ψ_{21} contain steps (3)-(10), (12)-(16), (18), (20)-(27), (30)-(34), (37) and (38), forming the "basic" part of the mechanism. According to ψ_1 , the most influential reaction sequence is formed by (27), (20), (3) and (4). This "reaction kernel" emphasizes that the largest effect is brought about by setting the parameters j_{27} and k_{20} . Also the NO/NO₂ ratio (Figs. 6 and 7) largely affects the simulated results. Due to the coupling of the individual reactions, this ratio not only depends on the rate of reactions (20) and (27) but also on all the reactions involving NO_x. Since j_{27} is an estimated parameter, some deviations of the simulated results may be attributed to it. An uncertainty analysis of this parameter shows that a change of 10% in

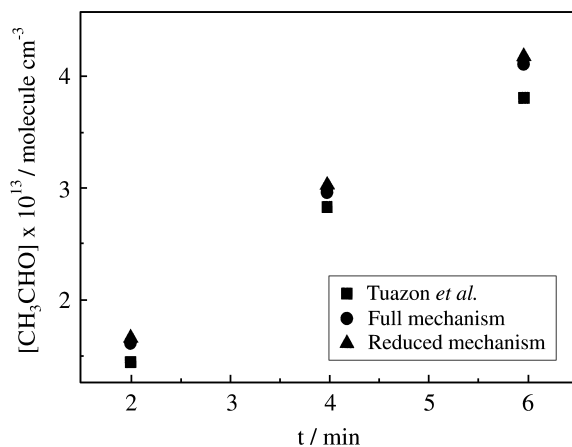


Figure 4. Simulated and experimental data for the acetaldehyde concentrations as a function of reaction time.

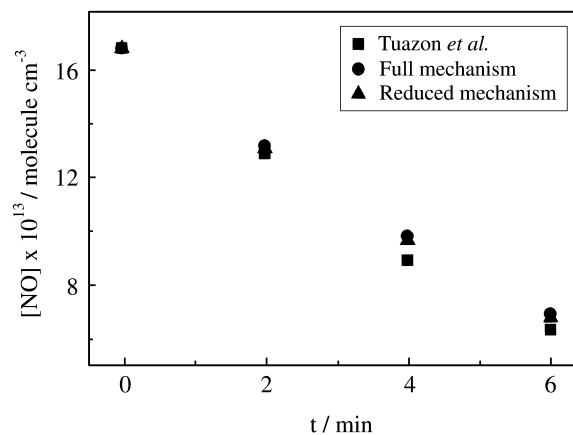


Figure 6. Simulated and experimental data for the NO concentrations as a function of reaction time.

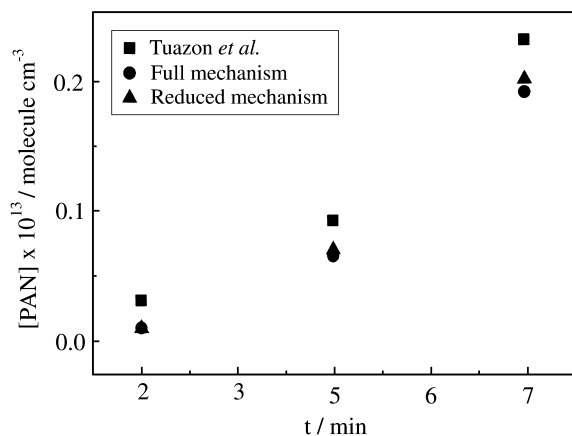


Figure 5. Simulated and experimental data for the peroxyacetyl nitrate (PAN) concentrations as a function of reaction time.

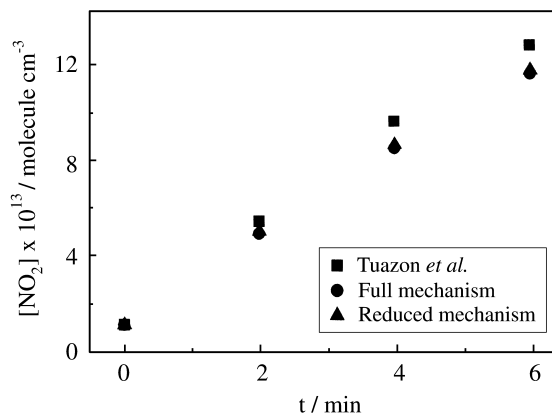


Figure 7. Simulated and experimental data for the NO₂ concentrations as a function of reaction time.

j_{27} leads to a substantial change of all product concentrations (6.8% in TBF and about 7.5% in the minor products). The inclusion of another minor reaction path, such as the formation of alkylnitrates, might affect the NO/NO_x ratios in a non-negligible amount.

2) According ψ_{22} to ψ_{27} , reactions (1), (2), (11) and (35), are of "transitional" importance. As it will be shown, in spite of their small contributions they can not be removed from the mechanism.

3) Reactions (17), (19), (28), (29), (36), (39), (40) and (41) contained in ψ_{28} to ψ_{41} with eigenvalues below 1.80×10^{-2} are unimportant and can be eliminated.

As shown in Table 4, eliminating the last group of reactions causes small changes in concentrations. However, additional elimination of steps (1), (2), (11) and (35) (*i.e.* reactions of "transitional" importance) leads to large deviations (Table 4). That is, no further reduction of the mechanism is possible since all concentration changes should be small. Table 4 also shows that the importance or contribution of individual reactions changes as the overall reaction proceeds.

The rank of reactions by overall sensitivity (Table 2) suggests that reactions (11) and (35) may be eliminated. However, this elimination leads to large deviations (*e.g.* at $t = 6$ min the deviation for HCHO is about 20%). On the other hand, reactions (19) and (28) with larger overall sensitivities can be dropped. The probable reason for this is that reactions (11) and (35) are coupled with other important reactions (see ψ_{24} - ψ_{27}).

The rate reaction rank (Table 2) gives a different rank of reactions and is not an effective way of reducing a mechanism. Individual rates do not consider the interactions between reactions and may lead to incorrect conclusions about the relevance of individual reactions. Anyway,

Table 4. Comparison of concentration deviations from full mechanism, eliminating of steps 17, 19, 28, 29, 36, 39, 40 and 41 (column A) and also steps 1, 2, 11 and 35 (column B).

Compounds	Deviations (%)	
	A	B
MTBE	-0.11	-0.52
TBF	1.52	7.24
HCHO	3.18	25.21
Methyl Acetate	1.52	7.25
Acetone	1.52	7.25
Ethyl Nitrite	-0.42	-0.42
NO	-2.15	-6.91
NO ₂	1.48	1.17
Acetaldehyde	1.82	0.47
PAN	6.79	16.67

as previously shown the rate of production analysis is a good method for the exploration of the reaction pathways.

Conclusions

The mechanism of Table 1 is quite successful in reproducing chamber data for the oxidation of MTBE by OH radicals. The rate of production analysis gives useful information in determining the main reaction pathways.

Principal component analysis shows that reactions are strongly coupled and confirms that the most influential reactions paths are the ethyl nitrite photolysis, the MTBE oxidation and the chemistry of NO_x and OH radical. On the basis of the calculated eigenvalues, the mechanism can be reduced to 33 reactions. No further reduction is possible since all concentration changes should be small. Certainly, the conclusions taken from the eigenvalue-eigenvector analysis are only valid for the rather narrow range of conditions of the smog chamber experiments. Anyway, the information seems useful to identify a minimal reaction set and to assess the relationships and dependencies among the parameters.

Acknowledgements

The authors gratefully acknowledge CAPES and FAPERJ for partial financial support, NCE/UFRJ for computing facilities on the SP2 supercomputer, and Prof. T. Turányi (Central Research Institute for Chemistry, Budapest, Hungary) for a free copy of KINAL package.

Note

All calculations were performed using the KINAL package³⁹.

References

- Dickinson, R.P.; Gelinas, R.J. *J. Comp. Phys.* **1976**, *21*, 123.
- Hwang, J.T.; Dougherty, E.P.; Rabitz, S.; Rabitz, H. *J. Chem. Phys.* **1978**, *69*, 5180.
- Dougherty, E.P.; Hwang, J.T.; Rabitz, H. *J. Chem. Phys.* **1979**, *71*, 1794.
- Edelson, D.; Allara, L. *Int. J. Chem. Kinet.* **1980**, *12*, 605.
- Turányi, T.; Bérces, T.; Vajda, S. *Int. J. Chem. Kinet.* **1989**, *21*, 83.
- Turányi, T. *J. Math. Chem.* **1990**, *5*, 203.
- Vajda, S.; Valko, P.; Turányi, T. *Int. J. Chem. Kinet.* **1985**, *17*, 55.
- Wallington, T.J.; Kurylo, M.J. *Int. J. Chem. Kinet.* **1987**, *19*, 1015.
- Tanner, R.L.; Miguel, A.H.; de Andrade, J.B.; Gaffney, J.S.; Streit, G.E. *Environ. Sci. Technol.* **1988**, *22*, 1026.

10. Wallington, T.J.; Andino, J.M.; Skewes, L.M.; Siegl, W.O.; Japar, S.M. *Int. Chem. Kinet.* **1989**, *21*, 993.
11. Anderson, E. V. *Chem. Eng. News* **1987**, *65*, 7.
12. Wallington, T.J.; Dagaut, P.; Liu, R.; Kurylo, M.J. *Environ. Sci. Technol.* **1988**, *22*, 842.
13. Cox, R.A.; Goldstone, A. In *Proceedings of the 2nd European Symposium on the Physical-Chemistry Behavior of Atmospheric Pollutants*, D. Riedel Publishing Co., Dordrecht, Holland, 1989, pp. 112-119.
14. Japar, S.M.; Wallington, T.J.; Richert, J.F.O.; Ball J.C. *Int. J. Chem. Kinet.* **1990**, *22*, 1257.
15. Grosjean, D.; Miguel, A.H.; Tavares, T.M. *Atmos. Environ.* **1990**, *24B*, 101.
16. Calvert, J.G. In *Some Considerations of the Mechanism of the Atmospheric Oxidation of MTBE and ETBE*, prepared for the Auto Oil Air Quality Improvement Research Program, Modeling Committee, March 8, 1990.
17. Chang, T.J.; Rudy, S.J. *Atmos. Environ.* **1990**, *24A*, 2421.
18. Smith, D.F.; Kleindienst, T.E.; Hudgens, E.E.; McIver, C.D.; Bufalini, J. J. *Int. J. Chem. Kinet.* **1991**, *23*, 907.
19. Tuazon, E.C.; Carter, W.P.L.; Aschmann, S.M.; Atkinson, R. *Int. J. Chem. Kinet.* **1991**, *23*, 1003.
20. Carter, W.P.L.; Tuazon, E.C.; Aschmann, S.M. In *Investigation of the Atmospheric Chemistry of Methyl tert-butyl ether (MTBE)*, prepared for the Auto/Oil Air Quality Improvement Research Program, January, 1991.
21. Langer, S.; Ljungström, E. *Int. J. Chem. Kinet.* **1994**, *26*, 367.
22. Atkinson, R. *J. Phys. Chem. Ref. Data* **1989**, Monograph n° 1, 1.
23. Atkinson, R. *J. Phys. Chem. Ref. Data* **1994**, Monograph n° 2, 1.
24. Atkinson, R. *Atmos. Environ.* **1990**, *24A*, 1.
25. Pimentel, A.S.; Arbilla, G. *Química Nova* **1997**, *20*, 252.
26. Harley, R.A.; Russell, A.G.; McRae, G.J.; Cass, G.R.; Seinfeld, J.H. *Environ. Sci. Technol.* **1993**, *27*, 378.
27. Leone, J.A.; Seinfeld, J.H. *Atmos. Environ.* **1988**, *19*, 437.
28. *Rethinking the Ozone Problem in Urban and Regional Air Pollution*, Committee on Tropospheric Ozone Formation and Measurement, National Academic Press, Washington, DC, 1991.
29. Carter, W.P.L. *Atmos. Environ.* **1990**, *24A*, 481.
30. Atkinson, R.; Baulch, D.L.; Cox, R.A.; Hampson Jr., R.F.; Kerr, J.A.; Troe, J. *J. Phys. Chem. Ref. Data* **1992**, *21*, 1125.
31. Atkinson, R.; Baulch, D.L.; Cox, R.A.; Hampson Jr., R.F.; Kerr, J.A.; Troe, J. *J. Phys. Chem. Ref. Data* **1989**, *18*, 881.
32. Atkinson, R. *Int. J. Chem. Kinet.* **1997**, *29*, 99.
33. Steinfeld, J.I.; Francisco, J.S.; Hase, W.L. In *Chemical Kinetics and Dynamics*, Prentice-Hall, Englewood Cliffs, NJ, 1989.
34. Pilling, M.J. *Modern Gas Kinetics*, Pilling, M.J.; Smith, I.W.M., eds., Blackwell, Oxford, 1987.
35. Hirst, D.M. In *A Computational Approach to Chemistry*, Blackwell Scientific Publications, Oxford, 1990.
36. Gelinas, R.J. Science Applications, Inc., Preprint No AI/PL/C279, 1979.
37. Kee, R.J.; Gear, J.F.; Smooke, M.D.; Miller, J.A. Sandia National Labs., SAND 85-8240, 1985.
38. Gardiner, Jr., W.C. *J. Phys. Chem.* **1977**, *81*, 2367.
39. Turányi, T. *Comp. Chem.* **1990**, *14*, 253-254.